Pergamon

Tetrahedron: Asymmetry, Vol. 7, No. 5, pp. 1309-1322, 1996

0957-4166/96 $15.00 + 0.00

S0957-4166(96)00148-6

STEREOCONTROL OF BILIRUBIN CONFORMATION

Stefan E. Boiadjiev and David A. Lightner*

Department of Chemistry, University of Nevada, Reno, Nevada 89557-0020 USA

Abstract: Optically active, diastereomeric synthetic bilirubin analogs (**1** and **2**) with an α-methyl and a β-methyl in each propionic acid side chain were synthesized. Both diastereomers adopt a folded, ridge-tile conformation. The methyls force the pigment to adopt either a left-handed (***M***) or right-handed (***P***) helicity. As evidenced by exciton-type circular dichroism spectra, in the ($\alpha S,\alpha' S,\beta S,\beta' S$) diastereomer (**1**) the ***M*** helicity ridge-tile enantiomer is strongly preferred; in the ($\alpha R,\alpha' R,\beta S,\beta' S$) diastereomer (**2**),the ***P*** helicity conformation is preferred.

INTRODUCTION

Bilirubin (Fig. 1) is a tetrapyrrole dicarboxylic acid formed in the normal metabolism of heme proteins.[1-3] In a healthy adult, it is produced at the rate of ~300 mg/day, principally from the breakdown of red blood cells. Bilirubin is intrinsically unexcretable but is efficiently eliminated by the liver following uptake and enzymic conversion to water-soluble glucuronides that are promptly secreted into bile. Impaired excretion of the glucuronides occurs in many types of hepatobiliary disease, but retention of native bilirubin is principally observed in newborn babies.[1-3] Accumulation of either native bilirubin or its glucuronides in the body is manifested in jaundice.

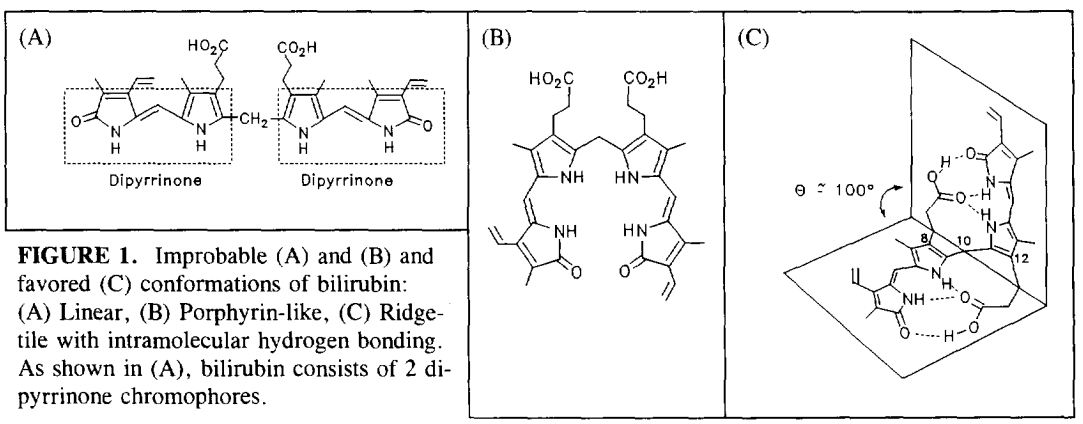

FIGURE 1. Improbable (A) and (B) and favored (C) conformations of bilirubin: (A) Linear, (B) Porphyrin-like, (C) Ridge-tile with intramolecular hydrogen bonding. As shown in (A), bilirubin consists of 2 dipyrrinone chromophores.

Bilirubin belongs to the class of pigments called "linear tetrapyrroles"; yet, its solution and biological properties do not correlate well with either the linear (Fig. 1A) or even a porphyrin-like (Fig. 1B) shape in which the polar carboxyl and lactam groups are freely solvated.[1,3] Its preferred shape is now known to be neither linear nor porphyrin-like, which are sterically disfavored conformations.[4] Rather, bilirubin is bent in the middle and adopts the shape of a half-opened book or a ridge-tile (Fig. 1C). In this conformation the propionic acid groups readily engage in intramolecular hydrogen bonding to the opposing dipyrrinone lactam and pyrrole components.[4] In bilirubin and its congeners with propionic acids at C(8) and C(12), this provides considerable conformational stabilization of the ridge-tile shape while tucking the polar groups inward and rendering the pigment surprisingly lipophilic.[5]

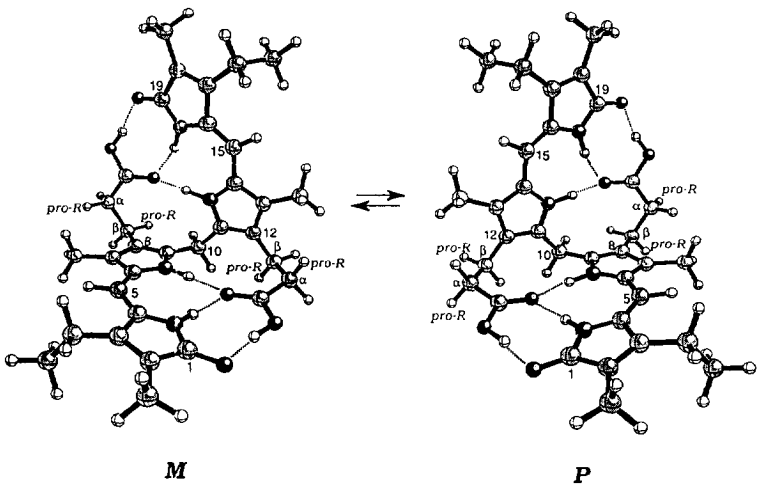

FIGURE 2. Ball and stick models of folded intramolecularly hydrogen-bonded mesobilirubin-XIIIα.

The ridge-tile conformation with its near-C_2-symmetry is dissymmetric; so, the conformation shown in Fig. 1C has a nonsuperimposable mirror image. Bilirubin (Fig. 1) and its analog mesobilirubin-XIIIα (Fig. 2) are thus a 50:50 mixture of conformational enantiomers, which equilibrates in solution (as illustrated in Fig. 2).[4] Displacement of the equilibrium toward one or the other of the enantiomers can be achieved by complexation with a chiral compound, such as quinine[6] or serum albumin,[7] and observed by circular dichroism (CD) spectroscopy. Selective stabilization of one enantiomer can also be achieved through intramolecular nonbonded steric interactions, as has been observed when stereogenic centers are created by methyl substitution at either the α or the β carbons of the propionic acid chains.[8,9] Such "intramolecular resolution" is the subject of the current work, with focus on two new diastereomeric analogs (**1** and **2**) of bilirubin that are designed to probe how methyl substitution influences the conformation equilibrium displayed in Figure 2.

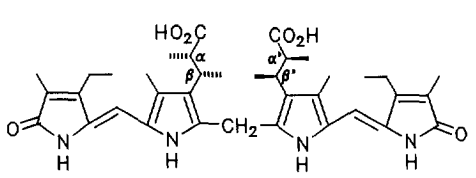

1: (α*S*,α'S,β*S*,β'*S*)-Tetramethyl-mesobilirubin-XIIIα

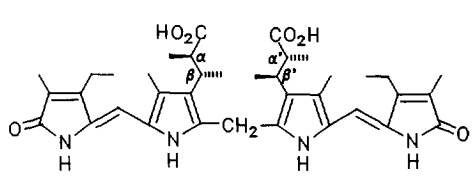

2: (α*R*,α'*R*,β*S*,β'*S*)-Tetramethyl-mesobilirubin-XIIIα

SYNTHETIC SCHEME

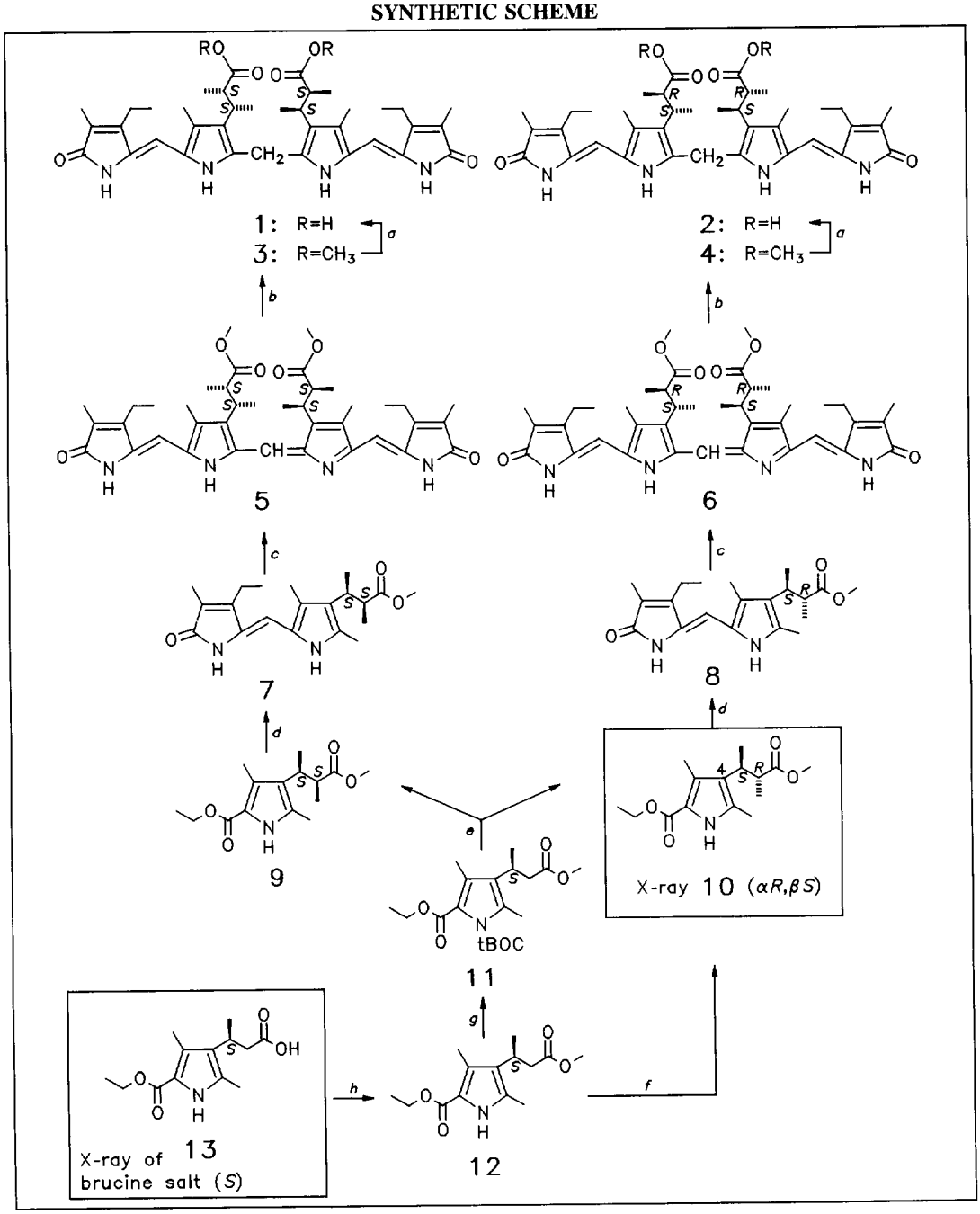

[a] $NaOH/H_2O$, then HCl; [b] $NaBH_4$, CH_3OH, THF; [c] *p*-chloranil, HCOOH; [d] $NaOH/H_2O$, then HNO_3, then 5-bromomethylene-4-ethyl-3-methyl-2-oxo-1*H*-pyrrole; [e] LDA, CH_3I, then CF_3COOH; [f] LDA, CH_3I; [g] $O[CO_2C(CH_3)_3]_2$, Et_3N, DMAP; [h] CH_2N_2.

RESULTS AND DISCUSSION

Synthesis. Bilirubin analogs **1** and **2** were prepared from the diastereomeric dipyrrinones **7** and **8** as outlined in the Synthetic Scheme, first by oxidative coupling[10] to verdin dimethyl esters **5** and **6** using *p*-chloranil, then reduction to the corresponding rubin dimethyl esters **3** and **4**, and finally saponification. Optically active dipyrrinones **7** and **8** of known absolute configuration had been prepared previously[11] by the route outlined. The key starting material was monopyrrole **13**, which was prepared and resolved as its brucine salt.[8] Its absolute configuration was determined by X-ray crystallography to be *S*.[8] Alkylation of the *t*-BOC derivative (**11**) of its methyl ester (**12**) gave two diastereomeric α,β-dimethyl derivatives, **9** and **10**, and the relative configuration of **10** was shown to be erythro by X-ray and ^{1}H-NMR analyses.[11] Since **13** was determined to have the βS configuration, **10** must be $\alpha R,\beta S$, and thus **9** has $\alpha S,\beta S$ configuration.

Structure and ^{13}C-NMR Spectra. The ^{13}C-NMR data (Table 1) for diastereomeric rubins **1** and **2** are consistent with the assigned structures. The data are compared in $(CD_3)_2SO$ solution, where both **1** and **2** are soluble. Although **1** is sufficiently soluble in $CDCl_3$; interestingly, its diastereomer **2** is too insoluble to obtain a ^{13}C-NMR spectrum. Not surprisingly, the ^{13}C-NMR spectra are very similar, with the most noticeable difference occurring in the chemical shifts of the β-CH_3 groups and lesser differences in the C(10)-CH_2- and in nearby ring carbons. Thus, although dimethylsulfoxide appears to exert a levelling effect on the data by interfering with the intramolecular hydrogen bonding that stabilizes pigment conformation, small yet potentially significant differences can be detected by ^{13}C-NMR.

Larger differences appear in the ^{13}C-NMR data of dimethyl esters **3** and **4** in $CDCl_3$. Although the data are consistent with the assigned structures and are qualitatively similar, chemical shift differences as large as ~2 ppm can be detected. For example, in **3** the lactam carbonyls at 1 and 19, the methyls at 2 and 18, meso carbons 5 and 15, and ring carbons 9 and 11 are all 1-2 ppm more shielded than the corresponding carbons in **4**. The greatest difference lies with *meso* carbons 5 and 15 (but not 10). Interestingly, the carbons cited are remote from the stereogenic centers, α and β, where the greatest stereodifferentiation occurs. The data suggest different conformations and differing extents of dimerization. (Bilirubin dimethyl esters are thought to form dimers in $CDCl_3$ through intermolecular hydrogen bonding.[12])

^{1}H-NMR and Hydrogen Bonding. The ^{1}H-NMR data (Table 2) for diastereomeric rubins **1** and **2** in $CDCl_3$ are quite similar in most respects. Significantly, the lactam, pyrrole and carboxylic acid chemical shifts, which have been shown to be excellent diagnostics for detecting intramolecular hydrogen bonding,[8,12,13] clearly indicate that **1** and **2** favor the ridge-tile conformations shown in Figs. 1 and 2. As might be expected, the diastereotopic α and β methyls exhibit different chemical shifts, and the ~0.5 ppm difference in chemical shift of the C(10) -CH_2- suggests that **1** and **2** do not adopt identical ridge-tile shapes.

In contrast, the ^{1}H-NMR data for dimethyl esters **3** and **4** are very different. In particular, attention is called to the differing sets of N-H chemical shifts. In **3** the more shielded pyrrole N-*H* resonance, like those in **1** and **2**, are an indicator of a folded conformation where one pyrrole N-*H* lies above the π-system of the other, as in Figs. 1 and 2. However, the accompanying lactam N-*H* is not as deshielded as in **1** and **2**, suggesting weaker intramolecular hydrogen bonding. In **4** both N-*H* resonances are more deshielded than in **3** and are more similar to those seen in mesobilirubin-XIIIα dimethyl ester and etiobilirubin-IVγ which form intermolecularly hydrogen-bonded dimers in chloroform solvent.[13]

TABLE 1. ^{13}C-NMR Assignments for Diastereomeric α,α′,β,β′-Tetramethylmesobilirubins **1** and **2** and Their Dimethyl Esters **3** and **4**.

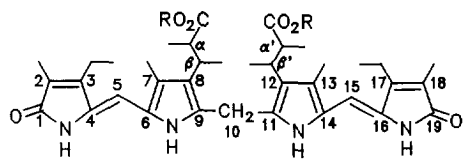

Carbon	R=H		R=CH_3	
	1[a] (αS,α′S,βS,β′S)	**2**[a] (αR,α′R,βS,β′S)	**3**[b] (αS,α′S,βS,β′S)	**4**[b] (αR,α′R,βS,β′S)
1,19-CO	172.1	172.0	173.1	174.2
2,18	122.7	122.6	124.0	123.5
2,18-CH_3	10.67	10.77	10.30	11.21
3,17	147.3	147.2	147.4	147.0
3,17-CH_2CH_3	14.89	14.84	14.79	14.71
3,17-CH_2CH_3	17.16	17.15	17.84	17.75
4,16	127.5	128.1	128.7	129.0
5,15	97.73	97.53	97.86	99.75
6,14	122.1	121.7	123.2	121.6
7,13	122.1	121.4	121.3	121.5
7,13-CH_3	8.10	8.08	8.18	7.61
8,12	123.3	123.0	124.1	124.5
β,β′-CH	33.50	33.41	34.73	34.79
β,β′-CH_3	16.65	18.86	18.53	19.27
α,α′-CH	44.19	44.14	46.60	45.36
α,α′-CH_3	16.27	16.55	16.57	16.76
α,α′-CO	177.3	177.6	178.4	177.4
9,11	130.8	130.4	130.1	131.3
10-CH_2	24.15	23.57	23.31	23.14
-OCH_3	—	—	52.73	51.42

[a] $(CD_3)_2SO$ solution. Values reported for 10^{-2} M solutions in ppm downfield from $(CH_3)_4Si$; [b] $CDCl_3$ solution.

These conclusions are supported by the HPLC retention times on a reverse phase column: **1**, retention time 151 min; **2**, 41 min; and **3**, 8.4 min; **4**, 6.6 min. Typically, on reverse phase HPLC, the more polar pigment elutes faster. Acids **1** and **2** are less polar than esters **3** and **4** due to their extensive intramolecular hydrogen bonding. Acid **2** is more polar than **1** due to less effective hydrogen bonding. And ester **3** is less polar than **4**, suggesting more effective hydrogen bonding.

TABLE 2. ^{1}H-NMR Assignments for Diastereomeric $\alpha,\alpha',\beta,\beta'$-Tetramethylmesobilirubins **1** and **2** and Their Dimethyl Esters **3** and **4** in $CDCl_3$.

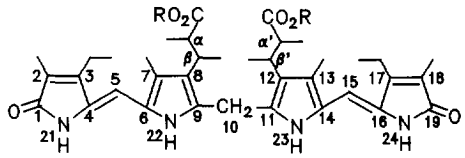

Proton	R=H		R=CH_3	
	1 ($\alpha S,\alpha' S,\beta S,\beta' S$)	**2** ($\alpha R,\alpha' R,\beta S,\beta' S$)	**3** ($\alpha S,\alpha' S,\beta S,\beta' S$)	**4** ($\alpha R,\alpha' R,\beta S,\beta' S$)
2,18-CH_3	1.84[a]	1.86[a]	1.75[g]	1.38[a]
3,17-CH_2CH_3	1.12[b]	1.11[h]	1.11[b]	0.98[b]
3,17-CH_2CH_3	2.47[c]	2.48[i]	2.45[c]	2.31[c]
5,15-CH=	6.04[a]	6.05[a]	5.92[a]	5.90[a]
7,13-CH_3	2.22[a]	2.10[a]	2.13[g]	2.16[a]
β,β'-CH	3.10-3.13[d]	3.03[j]	2.94-3.00[d]	3.10[n] 3.13
β,β'-CH_3	1.28[e]	1.62[k]	1.36[f]	1.35[o]
α,α'-CH	3.10-3.13[d]	2.94[j]	2.94-3.00[d]	2.77[p] 2.80
α,α'-CH_3	1.43[f]	1.49[k]	1.33[l]	0.90[l]
10-CH_2	4.02[a]	4.50[a]	4.04[g]	4.16[a]
21,24-NHCO	10.58[g]	10.61[g]	9.60[g]	10.75[g]
22,23-NH	8.90[g]	9.08[g]	9.03[m]	10.16[g]
-$COOCH_3$	—	—	3.62[g]	3.75[a]
-COOH	13.55[g]	13.60[g]	—	—

[a] s; [b] t, J=7.6 Hz; [c] q, J=7.6 Hz; [d] unresolved m; [e] d, J=6.3 Hz; [f] d, J=6.0 Hz; [g] br.s; [h] t, J=7.4 Hz; [i] q, J=7.4 Hz; [j] m; [k] d, J=7.4 Hz; [l] d, J=6.8 Hz; [m] very br.s; [n] dq, J=11.0, 7.0 Hz; [o] d, J=7.0 Hz; [p] dq, J=11.0, 6.8 Hz.

Conformational Analysis. In **1** and **2** the ^{1}H-NMR data clearly indicate a predominance of intramolecularly hydrogen-bonded ridge-tile structures such as those in Fig. 2. Intramolecular allosteric effects of the methyl groups substituted on the propionic side chains of such ridge-tile structures are predicted to displace the conformational equilibrium toward the ***M*** isomer when the stereochemistry at α or β is *S*, and toward the ***P*** isomer when it is *R*.[5,8,9] As may be seen in the ball and stick stereodrawings of Fig. 2, substitution of a *pro-R* hydrogen by β-methyl induces a nonbonded steric repulsion between the methyl group and C(10) -CH_2- in the ***M***-chirality conformer, but not in the ***P***. Similarly substitution of the *pro-R* hydrogen by an α-methyl induces a nonbonded steric repulsion between the methyl group and a C(7) or C(13) ring methyl. Consequently, the ***M***-chirality diastereomer is predicted to be strongly favored over the ***P*** when the stereogenic centers are $\alpha S,\alpha' S,\beta S,\beta' S$ (as in **1**). Here, the conformational selection imposed by the *S* stereochemistry

at a β-carbon is reinforced by that of the *S* stereochemistry at an α-carbon. Less clear is the prediction for the $\alpha R,\alpha' R,\beta S,\beta' S$ diastereomer (**2**) where the nonbonded steric interactions created by the βS stereochemistry act in opposition to those created by the αR stereochemistry; *i.e.*, the $\beta S,\beta S'$ should favor the ***M***-chirality conformer, but the $\alpha R,\alpha' R$ should favor the ***P***.

Nuclear Overhauser Effect. Experimental evidence for a folded, ***M***-chirality conformation of rubin **1** in chloroform comes from $^1H\{^1H\}$ NOE measurements. In the most stable, ***M***-chirality conformation of the ($\alpha S,\alpha' S,\beta S,\beta' S$)-diastereomer (**1**), the β,β'-methines are brought into close proximity to the C(10) -CH_2- hydrogens and, indeed, a strong NOE is observed between signals at 4.02 ppm (C(10) -CH_2-) and 3.11 ppm (α- and β-methines). No NOE was found, however, between the C(7), C(13)-methyls (2.22 ppm) and the α,α'-methyls (1.43 ppm) which lie far apart in the ***M***-chirality conformation of **1**. The signals for the C(7), C(13) methyl groups (2.22 ppm), the α- and β-CHs (overlapped at 3.11 ppm) and the β,β'-methyls (1.28 ppm) are also related by a strong NOE. Other NOEs are found between the lactam and pyrrole NHs, between C(5), C(15) hydrogens and the C(3), C(17)-ethyl and C(7), C(13)-methyl groups, confirming that the dipyrrinones adopt a *syn-Z* conformation. Selective $^1H\{^1H\}$ decoupling of either the α- or β-CH_3 in **1** and **2** (in $CDCl_3$ with added 5% v/v C_6D_6) showed that in the propionic acid side chains, the vicinal methine coupling $^3J_{H\text{-}H}$ is small — 3.2-3.9 Hz, in contrast to the 10-11 Hz observed in dipyrrinones **7**, **8** or verdins **5**, **6**. This suggests a different propionic acid conformation in rubins **1** and **2** as compared with the freely rotating propionic side chains in verdins **5** and **6**.

Less conclusive are the NOE experiments on rubin **2**, because all effects found are very weak, except within dipyrrinone moieties. The protons of the β,β'-methyls (1.62 ppm) and the C(10) -CH_2- (4.50 ppm), as well as those of the α,α'-methines (2.94 ppm) and C(7), C(13)-methyls (2.10 ppm) are related by a weak NOE, pointing to a predominance of the ***P***-chirality conformer of ($\alpha R,\alpha' R,\beta S,\beta' S$)-**2** in chloroform.

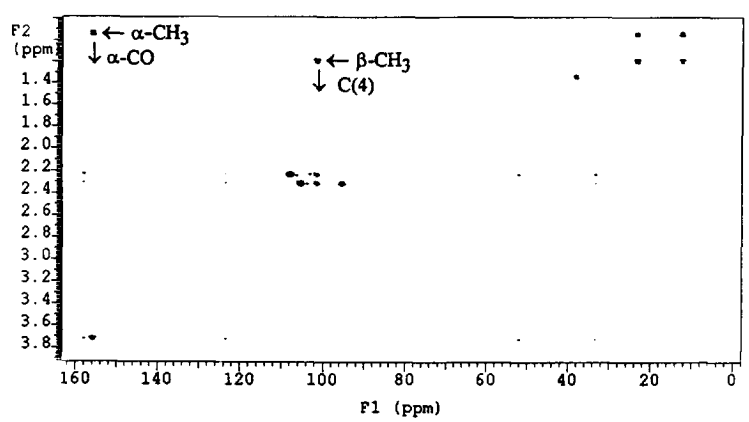

FIGURE 3. HMBC spectrum ($CDCl_3$) of the monopyrrole ($\alpha R,\beta S$)-**10** showing 3-bond coupling between the α-CH_3 and the propionic carboxyl carbon, and 3-bond coupling between the β-CH_3 and ring carbon 4. F2 is the ^{1}H-NMR scale, F1 is the ^{13}C-NMR.

The more shielded methyl group signal (0.94 ppm) in monopyrrole **10** belongs to an α-CH_3, the more deshielded (1.19 ppm) to a β-CH_3 — an assignment confirmed by HMBC-NMR correlation (Fig. 3). The relative shielding order in dimethyl ester **4** remains the same: the α-CH_3 lies at 0.90 ppm, the β-CH_3 at 1.35 ppm. No significant chemical shift difference was observed between monopyrrole **9** and the corresponding rubin dimethyl ester **3** (α-CH_3 at 1.21 ppm in **9**, at 1.33 ppm in **3** and β-CH_3 at 1.22 ppm in **9**, at 1.36 ppm in **3**). In mesobilirubin diacids **1** and **2**, which adopt an intramolecularly hydrogen-bonded conformation, the chemical shifts of the corresponding α and β methyls differ considerably,

due to van der Waals shielding (steric compression causes deshielding).[14] In **1**, the α-CH_3 is deshielded to 1.43 ppm and is thus more compressed than the β-CH_3. In **2**, although both α- and β-CH_3 groups lie 0.3-0.5 ppm downfield relative to the corresponding dimethyl ester (**4**), the β-methyls are more sterically compressed and shifted to 1.62 ppm. In the ***P***-chirality conformation of **2**, the βS-methyls lie near to the folding line (Figs. 1C and 2) and are compressed into the C(10) -CH_2- (see NOE experiments). The same deshielding effect, due to steric crowding, is clearly seen for the C(10) -CH_2- of **2**, where it is shifted from a normal value of 4.0-4.1 ppm to 4.5 ppm due to buttressing from the β,β'-CH_3s in the ***P***-chirality conformer.

Circular Dichroism and Stereochemistry. The effectiveness of the α and β methyls in displacing the conformational equilibrium of Fig. 2 may be detected and analyzed by circular dichroism (CD) spectroscopy. Intense bisignate CD Cotton effects (CEs) are observed for both **1** and **2** (Fig. 4 and Table 3). The origin of the observed CEs cannot be due simply to the introduction of stereogenic centers on the propionic acids of **1** and **2** because one would expect only a weak, monosignate CD associated with $\pi \rightarrow \pi^*$ excitation from a dipyrrinone chromophore perturbed by dissymmetric vicinal action.[11] Rather, the bisignate spectra are characteristic of an exciton system in which two chromophores interact by coupling locally excited $\pi \rightarrow \pi^*$ transitions (electric transition dipole coupling).[3] The component dipyrrinone chromophores of the bichromophoric rubins have strongly-allowed long-wavelength electronic transitions ($\Delta\epsilon_{410}^{max} \sim 37{,}000$) and only a small interchromophoric orbital overlap in the folded conformation (Figs. 1C and 2, dihedral angle $\simeq 100°$). They interact through resonance splitting, *i.e.*, by electrostatic interaction of the local transition moment dipoles, which are oriented along the long axis of each dipyrrinone.[3] Such intramolecular exciton splitting interaction produces two long wavelength transitions in the UV-vis spectrum and two corresponding bands in the CD spectrum. One band is higher in energy, and one is lower in energy, with the splitting being dependent on the strength and relative orientation of the dipyrrinone electric dipole transition moments. When observed by UV-vis spectroscopy, the two electronic transitions overlap to give the typically broadened and sometimes split long wavelength absorption band found in bilirubins. In the CD spectra, however, where the two exciton transitions are oppositely signed, bisignate CEs are typically seen — as predicted by theory.[3,15]

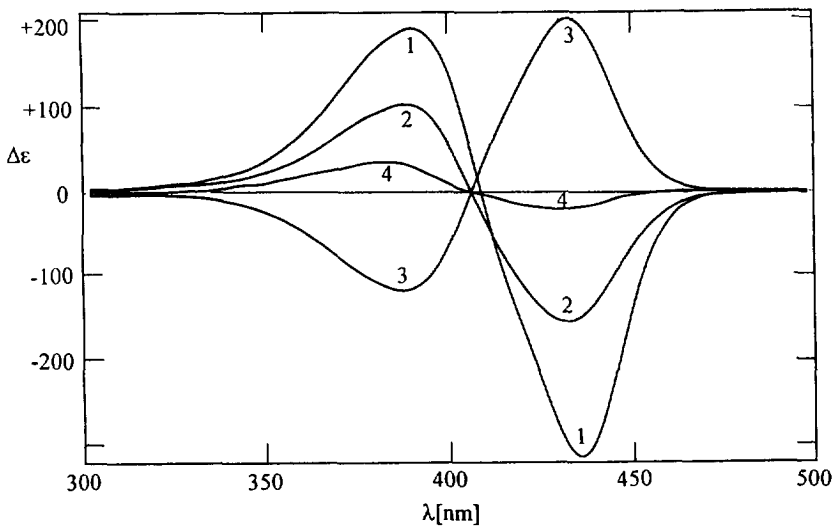

FIGURE 4. Circular dichroism of 1.5 x 10^{-5} M solutions of ($\alpha S,\alpha' S,\beta S,\beta' S$)-tetramethylmesobilirubin-XIIIα (**1**) in chloroform (spectrum 1), methanol (spectrum 2) and ($\alpha R,\alpha' R,\beta S,\beta' S$)-tetramethylmesobilirubin-XIIIα (**2**) in chloroform (spectrum 3), methanol (spectrum 4).

TABLE 3. Comparison of Circular Dichroism and UV Spectral Data from 1.5 x 10^{-5} M Solutions of Diastereomeric $\alpha,\alpha',\beta,\beta'$-Tetramethylmesobilirubin-XIIIα (**1** and **2**) at 22°C.

Pigment	Solvent	Dielectric Constant[a]	CD			UV			
			$\Delta\epsilon^{max}(\lambda_1)$	λ_2 at $\Delta\epsilon=0$	$\Delta\epsilon_{max}(\lambda_3)$	ϵ_{max}	λ(nm)	ϵ_{max}	λ(nm)
1	Cyclohexane	2.0	+176 (391)	405	−363 (432)	54,700	414	59,500	435
2			−104 (392)	406	+217 (433)	52,100	419^{sh}	58,900	436
1	CCl_4	2.2	+168 (392)	407	−342 (435)	52,700	419	57,000	437
2			− 98 (393)	408	+213 (435)	51,700	420^{sh}	57,600	439
1	Dioxane	2.2	+168 (388)	406	−292 (433)	54,100	416^{sh}	56,100	432
2			− 35 (393)	413	+ 33 (433)	42,500	384	39,400	414
1	Benzene	2.3	+186 (389)	406	−317 (433)	52,400	419^{sh}	54,200	433
2			− 99 (392)	408	+195 (435)	50,300	420^{sh}	54,700	437
1	$CHCl_3$	4.7	+193 (390)	409	−314 (436)			54,700	432
2			−118 (388)	407	+204 (433)			54,000	432
1	$ClCH_2CH_2Cl$	10.4	+180 (389)	408	−296 (434)			54,700	432
2			−104 (390)	408	+179 (434)			53,500	433
1	$(CH_3)_2CO$	20.7	+168 (386)	405	−279 (431)			54,800	426
2			+ 27 (366)	379	− 33 (397)	46,900	377	36,900	412^{sh}
				423	+9.4 (432)				
1	CH_3CH_2OH	24.3	+ 71 (399)	419	− 94 (440)			56,200	424
2			+ 48 (387)	416	− 18 (435)			61,700	433
1	CF_3CH_2OH	26.5	+151 (389)	409	−232 (436)			53,600	428
2			−8.3 (317)	342	+ 31 (393)			53,200	435
1	CH_3OH	32.6	+103 (388)	406	−155 (432)			56,200	422
2			+ 34 (384)	406	− 21 (430)	44,800	398^{sh}	58,300	430
1	CH_3CN	36.2	+163 (385)	404	−265 (429)			53,400	422
2			− 42 (391)	410	+ 45 (430)	40,400	375	37,900	420
1	$(CH_3)_2NCHO$	36.7	+131 (383)	401	−196 (424)	52,700	407^{sh}	57,100	423
2			+ 13 (377)	393	− 21 (424)	47,600	394^{sh}	51,900	420
1	$(CH_3)_2SO$	46.5	−5.0 (330)	349	+ 29 (427)	47,800	398^{sh}	60,100	430
2			+ 32 (380)	398	− 31 (426)	49,600	399^{sh}	54,900	426
1	Phosphate	(78)	+ 79 (378)	397	−129 (423)			57,600	422
2	Buffer, pH 7.4		− 4 (319)	356	+ 22 (401)	40,000	398^{sh}	41,200	420
1	Borate Buffer,	(78)	+ 79 (378)	397	−131 (423)			60,300	421
2	pH 9.5		− 4 (327)	358	+ 22 (404)	39,400	396^{sh}	40,500	420
1	CH_3NHCHO	181.2	+165 (384)	402	−267 (428)			63,000	427
2			+ 13 (383)	398	− 21 (431)	48,900	397^{sh}	52,200	423

[a] From Gordon, A.J.; Ford, R.A. *The Chemist's Companion*, Wiley, NY (1972), pp 4-9.

According to exciton chirality theory,[15] the signed order of the bisignate CD CEs may be used to predict the relative orientation of the two electric dipole transition moments, one from each dipyrrinone of the rubin. Thus, a positive exciton chirality (long wavelength (+) CE followed by a (−) short wavelength CE) corresponds to a positive torsion angle between the transition dipoles, and a negative exciton chirality (long wavelength (−) CE followed by a (+) short wavelength CE) corresponds to a negative torsion angle. The ***M***-helicity conformer of Fig. 2 is predicted to have a negative exciton chirality; the ***P***-helicity is predicted to have a positive exciton chirality.

In all solvents except $(CH_3)_2SO$, **1** exhibits a negative exciton chirality, suggesting a predominance of the *M*-helicity conformer and confirming the predictions drawn above and based on nonbonded intramolecular steric interactions in the $\alpha S,\alpha' S,\beta S,\beta' S$ diastereomer. The CD intensities are 70-90% of those seen in $\beta S,\beta' S$-dimethylmesobilirubin-XIIIα,[8] thus indicating that its conformational equilibrium (Fig. 2) is already displaced completely toward *M*, and any conformational reinforcement due to the αS and $\alpha' S$ methyls is not only redundant but is probably offset by the introduction of a new *gauche* butane interaction between the α and β methyls. In $(CH_3)_2SO$ solvent, where the CE intensity drops to $< 10\%$ of the maximum values — both in **1** and in $(\beta S,\beta' S)$-dimethylmesobilirubin-XIIIα,[8] it seems probable that the favored folded conformation has become somewhat more open to accommodate attachment of the solvent molecules.[16] As shown earlier,[3] flattening the ridge-tile leads to a reorientation of the dipyrrinone electric transition dipole moments to near parallelity (and hence to very weak bisignate CEs) and a change in torsion from (−) to (+) without a change in conformational chirality. In aqueous base the CEs remain strong, consistent with an *M* helicity dianion.

The CD data of $(\alpha R,\alpha' R,\beta S,\beta' S)$ diastereomer **2** contrast strongly with those of **1**. In nonpolar solvents such as cyclohexane and chloroform, **2** exhibits intense *positive* exciton chirality, consistent with the equilibrium of Fig. 2 being displaced toward *P*; whereas, the CD CEs of **1** are more intense with a *negative* exciton chirality due to a predominance of *M*. These data suggest that, on balance, the steric influence of the α-methyls counteracts and dominates that of the β-methyls when they work in opposition (in **2**). However, the dominance is not as effective in more polar solvents, where the CE intensities of **2** are far weaker than those of **1**. In solvents such as acetone and methanol, the β-methyls seem to dominate, but in most polar solvents the CD spectra of **2** is more complex than those of **1**, as if multiple species were present.

Dimethyl Esters. The UV spectra of **3** and **4** (Table 4) exhibit, like the parent acids **1** and **2**, characteristic exciton splitting of the long wavelength transition. The UV spectra of **3** and **4** differ, with the former being more like those of **1** and **2**, whose exciton bands are of nearly equal intensity. The latter, on the other hand have most of the intensity in the higher energy exciton component. Such data suggest that **3** and **4** adopt different conformations, that predominant conformation of **4** tends toward the porphyrin-like shape.

The CD spectra of **3** and **4** differ but are generally less intense than those of parent acids **1** and **2**. Diester **4** consistently exhibits negative exciton chirality CD; whereas, **3** exhibits variably negative and positive exciton chirality CD. The CD and UV data for **4** suggest a dominant positive helical conformation, probably in a dimer. On the other hand, the data for **3** are consistent with a folded conformation, similar to the ridge-tiles of Fig. 2, but with less hydrogen bonding and probably a more open conformation.

CONCLUDING COMMENTS

Intramolecular hydrogen bonding, which is characteristic of natural bilirubin and its analogs, is known to be a dominant force in determining their conformation. The current study shows that when the propionic acid residues are substituted with methyl groups at the α and β positions, thus creating stereogenic centers, mesobilirubin-XIIIα is forced by nonbonded steric interactions to adopt either the *M* or *P* helicity ridge tile conformation. When all α,β centers have the *S* configuration, the *M*-helicity conformer is dominant. However, when the non-bonded interactions operate in conflict, as in the $\alpha R,\beta S$ configuration, a more open *P*-helicity ridge-tile is suggested for nonpolar solvents. In this more open conformation, the observed exciton chirality CD is inverted relative to that of the $\alpha S,\beta S$ isomer.

TABLE 4. Comparison of Circular Dichroism and UV Spectral Data from 1.5 x 10^{-5} *M* Solutions of Diastereomeric $\alpha,\alpha',\beta,\beta'$-Tetramethylmesobilirubin-XIIIα Dimethyl Esters (**3** and **4**) at 22°C.

Pigment	Solvent	Dielectric Constant[a]	CD			UV			
			$\Delta\epsilon^{max}(\lambda_1)$	λ_2 at $\Delta\epsilon=0$	$\Delta\epsilon^{max}(\lambda_3)$	ϵ^{max}	λ(nm)	ϵ^{max}	λ(nm)
3	Cyclohexane	2.0	+ 39 (376)	390	− 50 (415)	59,100	380	38,200	410
4			+ 80 (369)	391	− 68 (435)	79,800	376	16,000	428^{sh}
3	CCl_4	2.2	+ 49 (378)	388	−116 (415)	47,800	394	52,100	417
4			+ 78 (372)	394	− 76 (437)	76,100	380	16,900	430^{sh}
3	Dioxane	2.2	+ 34 (374)	386	− 78 (412)	51,400	393	54,000	413
4			+ 75 (369)	391	− 71 (431)	71,600	377	23,600	419^{sh}
3	Benzene	2.3	+ 52 (375)	389	−102 (413)	65,700	394	48,600	413^{sh}
4			+ 86 (371)	391	− 86 (434)	77,400	378	16,000	432^{sh}
3	$CHCl_3$	4.7	− 26 (370)	383	+ 34 (410)	52,900	401^{sh}	55,400	416
4			+ 99 (369)	390	− 91 (427)	74,400	377	17,700	428^{sh}
3	Ethyl Acetate	6.0	+ 13 (376)	387	− 25 (412)	52,900	386	51,300	410
4			+ 94 (367)	388	− 81 (420)	78,800	374	17,700	424^{sh}
3	THF	7.3	+ 16 (375)	387	− 37 (413)	51,300	393	53,300	413
4			+ 76 (369)	390	− 70 (420)	74,400	375	24,500	418^{sh}
3	$ClCH_2CH_2Cl$	10.4	− 44 (371)	384	+ 66 (411)	50,500	394	52,600	413
4			+101 (369)	390	− 93 (430)	74,200	376	15,200	432^{sh}
3	$(CH_3)_2CO$	20.7	− 11 (367)	382	+ 13 (408)	51,500	390	52,000	411
4			+ 91 (367)	388	− 79 (421)	76,500	374	23,600	420^{sh}
3	CH_3CH_2OH	24.3	+ 11 (386)	403	−6.5 (417)			55,800	419
4			+ 36 (383)	402	− 29 (429)	49,800	397^{sh}	63,900	428
3	CF_3CH_2OH	26.5	− 50 (376)	396	+ 62 (423)			55,500	419
4			+ 18 (367)	398	− 21 (436)	47,700	389	45,600	413^{sh}
3	CH_3OH	32.6	+ 18 (376)	393	− 28 (417)			55,700	418
4			+ 22 (382)	396	− 29 (426)	49,000	394^{sh}	62,900	426
3	CH_3CN	36.2	− 11 (369)	382	+ 14 (409)	50,800	386	49,000	406
4			+ 95 (366)	387	− 84 (419)	78,900	373	18,600	420^{sh}
3	$(CH_3)_2NCHO$	36.7	− 15 (376)	390	+ 30 (419)	48,200	391	49,300	417
4			+ 22 (381)	400	− 32 (430)	53,200	389	56,900	419
3	$(CH_3)_2SO$	46.5	− 10 (381)	393	+ 27 (425)	46,100	396^{sh}	56,600	427
4			+ 25 (377)	395	− 31 (428)	50,300	395^{sh}	56,300	424
3	CH_3NHCHO	181.2	−9.7 (375)	394	+ 19 (423)	47,200	395	48,300	420
4			+ 20 (380)	395	− 31 (428)	50,300	395^{sh}	56,300	424

[a] From Gordon, A.J.; Ford, R.A. *The Chemist's Companion*, Wiley, NY (1972), pp 4-8.

EXPERIMENTAL

General. All UV-vis spectra were recorded on a Perkin Elmer model 3840 diode array or Cary 219 spectrophotometer, and all circular dichroism (CD) spectra were recorded on a JASCO J-600 instrument. NMR spectra were obtained on a GN-300 or Varian Unity Plus spectrometers operating at 300 MHz and 500 MHz, respectively. $CDCl_3$ solvent (unless otherwise noted) was used and chemical shifts were reported in δ ppm referenced to residual $CHCl_3$ ^1H signal at 7.26 ppm and ^{13}C signal at 77.00 ppm. J-modulated spin-echo experiment (*A*ttached *P*roton *T*est) was used to obtain ^{13}C-NMR spectra. Optical rotations were measured on a Perkin-Elmer model 141 polarimeter. HPLC analyses were carried out on a Perkin-Elmer Series 410

high-pressure liquid chromatograph with a Perkin-Elmer LC-95 UV-vis spectrophotometric detector (set at 420 nm) equipped with a Beckman-Altex ultrasphere IP 5μm C-18 ODS column (25 x 0.46 cm) kept at 35°C. The flow rate was 1.0 ml.min^{-1}. The mobile phase was 0.1 M di-n-octylamine acetate buffer in 5% aqueous methanol (pH 7.7 at 25°C). Gas chromatography (GC)- mass spectroscopy (MS) analyses were carried out on Hewlett-Packard 5890A capillary gas chromatograph (30 m DB-1 column) equipped with Hewlett-Packard 5970 mass selective detector. Radial chromatography was carried out on Merck Silica gel PF_{254} with $CaSO_4$ preparative layer grade, using a Chromatotron (Harrison Research, Inc., Palo Alto, CA). Melting points were determined on a Mel-Temp capillary apparatus and are uncorrected. Combustion analyses were carried out by Desert Analytics, Tucson, AZ.

Spectral data were obtained in spectral grade solvents (Aldrich or Fischer). Di-n-octylamine, formic acid, trifluoroacetic acid, 4-dimethylaminopyridine, *p*-chloranil (tetrachloro-1,4-benzoquinone), and sodium borohydride were from Aldrich. HPLC grade solvents (Fischer) were dried and distilled prior use: tetrahydrofuran (THF) from $LiAlH_4$, methanol from magnesium methoxide, dimethylsulfoxide from CaH_2, and dichloromethane from P_2O_5.

(-)-(1*S*,1′*S*,2*S*,2′*S*)-3,17-Diethyl-8,12-bis-(1,2-dimethyl-2-methoxycarbonylethyl)-2,7,13,18-tetramethyl-(21*H*,24*H*)-bilin-1,19-dione (α*S*,α′*S*,β*S*,β′*S*-tetramethylmesobiliverdin-XIIIα dimethyl ester) (5). A mixture of 344 mg (1 mmol) of dipyrrinone **7**, 615 mg, (2.5 mmol) of *p*-chloranil, 220 mL of dry CH_2Cl_2, and 11.5 mL of formic acid was heated at reflux for 24 h. The volume was reduced by one half by distillation and reflux continued for an additional 6 h. The mixture was kept overnight at −25°C and the separated solid was removed by filtration. The cold filtrate was carefully neutralized with sat. $NaHCO_3$. The organic layer was washed with 5% NaOH (3 x 70 mL), water until neutral (4 x 200 mL), dried (Na_2SO_4) and filtered. The solvent was removed under vacuum, and the crude product was purified by radial chromatography (2-3% CH_3OH in CH_2Cl_2) collecting the nonpolar bright blue band to afford **5** in 61% yield. It had mp 238-241°C, $[\alpha]_{436}^{20}$ -2480 (*c* 4.6 x 10^{-3}, $CHCl_3$). ^{1}H-NMR: δ 1.22 (t, 6H, J=7.6 Hz), 1.32 (d, 6H, J=6.8 Hz), 1.38 (d, 6H, J=7.2 Hz), 1.82 (s, 6H), 2.14 (s, 6H), 2.51 (q, 4H, J=7.6 Hz), (2.84, 2.87) (dq, 2H, J=9.9, 6.8 Hz), (3.18, 3.22) (dq, 2H, J=9.9, 7.2 Hz), 3.48 (s, 6H), 5.97 (s, 2H), 6.90 (s, 1H), 7.93 (br. s, 2H) ppm; ^{13}C-NMR: δ 8.31, 10.43, 14.47, 15.71, 17.58, 17.88, 34.40, 45.80, 51.56, 96.25, 115.7, 127.6, 128.1, 139.4, 140.5, 141.6, 146.9, 149.8, 172.1, 176.0 ppm.

Anal. Calcd. for $C_{39}H_{50}N_4O_6$ (670.8): C, 69.82; H, 7.51; N, 8.35
Found: C, 69.85; H, 7.36; N, 8.19

(+)-(1*S*,1′*S*,2*R*,2′*R*)-3,17-Diethyl-8,12-bis-(1,2-dimethyl-2-methoxycarbonylethyl)-2,7,13,18-tetramethyl-(21*H*,24*H*)-bilin-1,19-dione (α*R*,α′*R*,β*S*,β′*S*-tetramethylmesobiliverdin-XIIIα dimethyl ester) (6). This verdin was synthesized from **8** in 69% yield as above. It had mp 263-265°C, $[\alpha]_{436}^{20}$ +1350 (*c* 3.1 x 10^{-3}, $CHCl_3$). ^{1}H-NMR: δ 1.03 (d, 6H, J=6.9 Hz), 1.23 (t, 6H, J=7.6 Hz), 1.35 (d, 6H, J=7.1 Hz), 1.83 (s, 6H), 2.15 (s, 6H), 2.53 (q, 4H, J=7.6 Hz), (2.81, 2.84) (dq, 2H, J=10.8, 6.9 Hz), (3.14, 3.18) (dq, 2H, J=10.8, 7.1 Hz), 3.78 (s, 6H), 6.00 (s, 2H), 6.90 (s, 1H), 7.89 (br.s, 2H) ppm; ^{13}C-NMR: δ 8.32, 10.44, 14.45, 16.86, 17.90, 19.68, 34.80, 45.72, 51.69, 96.00, 114.9, 127.8, 128.2, 139.7, 140.8, 140.8, 147.0, 150.1, 172.0, 176.7 ppm.

Anal. Calcd. for $C_{39}H_{50}N_4O_6$ (670.8): C, 69.82; H, 7.51; N, 8.35
Found: C, 69.53; H, 7.43, N, 8.30

(+)-(1*S*,1′*S*,2*S*,2′*S*)-3,17-Diethyl-8,12-bis-(1,2-dimethyl-2-methoxycarbonylethyl)-2,7,13,18-tetramethyl-(10*H*,21*H*,23*H*,24*H*)-bilin-1,19-dione (α*S*,α′*S*, β*S*,β′*S*-tetramethylmesobilirubin-XIIIα dimethyl ester) (3). Purified verdin dimethyl ester **5** (0.2 mmol) was dissolved in 35 mL of dry N_2-saturated THF. While bubbling N_2 through the solution, 0.76 g (20 mmol) of $NaBH_4$ was added followed by 15 mL of dry CH_3OH added dropwise over 15 min. The reaction was quenched with 100 mL of H_2O, and the mixture was slowly acidified at 0°C with 10% HCl. The product was extracted with $CHCl_3$ (4 x 20 mL), washed with H_2O until neutral, dried (Na_2SO_4) and filtered. The solvent was removed under vacuum, and the crude product was purified by radial chromatography (3% MeOH in CH_2Cl_2). After evaporation of the collected bright yellow band, it was recrystallized from a minimum volume of $CHCl_3$ and five-fold volume of CH_3OH added portion wise to afford **3** in 62% yield. It had mp 233-236°C (decomp.), $[\alpha]_D^{20}$ +120 (*c* 4 x 10^{-2}, $CHCl_3$); ^1H and ^{13}C-NMR see Tables 1 and 2.

Anal. Calcd. for $C_{39}H_{52}N_4O_6$ (672.8): C, 69.61; H, 7.79; N, 8.33
Found: C, 69.85; H, 7.57; N, 8.25

(-)-(1*S*,1′*S*,2*R*,2′*R*)-3,17-Diethyl-8,12-bis-(1,2-dimethyl-2-methoxycarbonylethyl)-2,7,13,18-tetramethyl-(10*H*,21*H*, 23*H*,24*H*)-bilin-1,19-dione (α*R*,α′*R*,β*S*,β′*S*-tetramethylmesobilirubin-XIIIα dimethyl ester) (4). This rubin ester was prepared as above from **6** in 85% yield. It had mp 268-270°C (decomp.), $[\alpha]_D^{20}$ −3210 (*c* 4 x 10^{-3}, $CHCl_3$); ^1H and ^{13}C-NMR see Tables 1 and 2.

Anal. Calcd. for $C_{39}H_{52}N_4O_6$ (672.8): C, 69.61; H, 7.79; N, 8.33
Found: C, 69.39; H, 7.69; N, 8.37

(−)-(1*S*,1′*S*,2*S*,2′*S*)-8,12-bis-(2-Carboxy-1,2-dimethylethyl)-3,17-diethyl-2,7,13,18-tetramethyl-(10*H*, 21*H*, 23*H*,24*H*)-bilin-1,19-dione (αS,α′S,βS,β′S-tetramethylmesobilirubin-XIIIα) (1). A mixture of 50 μmol of rubin dimethyl ester **3**, 10 mL of EtOH, and 1 mL of 1N NaOH was heated at reflux under N_2 for 1.5 h. The mixture was diluted with 50 mL of H_2O and acidified with 10% HCl to pH ~ 3. The product was extracted with $CHCl_3$ (4 x 20 mL), washed with H_2O (2 x 50 mL), dried (Na_2SO_4) and filtered. The solvent was removed under vacuum, and the crude product was purified by radial chromatography (3-5% CH_3OH in CH_2Cl_2). The bright yellow band was collected, evaporated and recrystallized from CH_3OH-Et_2O or minimum volume of $CHCl_3$ and CH_3OH added dropwise to afford **1** in 58% yield. It had mp 294-297°C (decomp.), $[\alpha]_D^{20}$ −5710 (*c* 4.6 x 10^{-3}, $CHCl_3$); ^1H and ^{13}C-NMR see Tables 1 and 2.

Anal. Calcd. for $C_{37}H_{48}N_4O_6$ (644.8): C, 68.92; H, 7.50; N, 8.69
Found: C, 68.89; H, 7.24; N, 8.39

(+)-(1*S*,1′*S*, 2*R*,2′*R*)-8,12-bis-(2-Carboxy-1,2-dimethylethyl)-3,17-diethyl-2,7, 13, 18-tetramethyl-(10*H*, 21*H*, 23*H*, 24*H*)-bilin-1,19-dione (α*R*,α′*R*,β*S*,β′*S*-tetramethylmesobilirubin-XIIIα) (2). This rubin was prepared from **4** in 44% yield. It had mp 261-264°C (decomp.), $[\alpha]_D^{20}$ +3760 (*c* 5.9 x 10^{-4}, $CHCl_3$); ^1H and ^{13}C-NMR see Tables 1 and 2.

Anal. Calcd. for $C_{37}H_{48}N_4O_6$ (644.8): C, 68.92; H, 7.50; N, 8.69
Found: C, 69.09; H, 7.28; N, 8.45.

Acknowledgement: We thank the National Institutes of Health (HD 17779) for generous support of this work and the National Science Foundation (CHE-9214294) for assistance in purchasing the 500 MHz NMR spectrometer used in this work. S.E. Boiadjiev is on leave from the Institute of Organic Chemistry, Bulgarian Academy of Sciences, Sofia.

REFERENCES

1. McDonagh, A.F. In *The Porphyrins*; Dolphin, D., ed.; Academic Press: New York, **1979**, *6*, 293-491.
2. Ostrow, J.D., ed.; *Bile Pigments and Jaundice*; Marcel-Dekker: New York, **1986**.
3. Lightner, D.A.; McDonagh, A.F. *Accounts Chem. Res.* **1984**, *17*, 417-424.
4. Person, R.V.; Peterson, B.R.; Lightner, D.A. *J. Am. Chem. Soc.* **1994**, *116*, 42-59.
5. McDonagh, A.F.; Lightner, D.A. *Pediatrics* **1985**, *75*, 443-455.
6. Lightner, D.A.; Gawroński, J.K.; Wijekoon, W.M.D. *J. Am. Chem. Soc.* **1987**, *109*, 6354-6362.
7. Lightner, D.A.; Wijekoon, W.M.D.; Zhang, M.H. *J. Biol. Chem.* **1988**, *263*, 16669-16676.
8. Boiadjiev, S.E.; Person, R.V.; Puzicha, G.; Knobler, C.; Maverick, E.; Trueblood, K.N.; Lightner, D.A. *J. Am. Chem. Soc.* **1992**, *114*, 10123-10133.
9. Puzicha, G.; Pu, Y-M.; Lightner, D.A. *J. Am. Chem. Soc.* **1991**, *113*, 3583-3592.
10. Shrout, D.P.; Lightner, D.A. *Synthesis* **1990**, 1062-1065.
11. Boiadjiev, S.E.; Anstine, D.T.; Maverick, E.; Lightner, D.A. *Tetrahedron: Asymmetry* **1995**, *6*, 2253-2270.
12. For leading references, see: Falk, H. *The Chemistry of Linear Oligopyrroles and Bile Pigments*; Springer Verlag: NY, **1989**.
13. (a) Trull, F.R.; Ma, J.S.; Landen, G.L.; Lightner, D.A. *Israel J. Chem.* **1983**, *23 (2)*, 211-218.
    (b) Lightner, D.A.; Trull, F.R. *Spectroscopy Lett.* **1983**, *16*, 785-803.
    (c) Lightner, D.A.; Ma, J-S. *Spectroscopy Lett.* **1984**, *17*, 317-327.
14. For leading references, see Jackman, L.M.; Sternhell, S. *Applications of Nuclear Magnetic Resonance Spectroscopy in Organic Chemistry*, 2nd Ed., Pergamon Press, Oxford, **1969**, pages 71 and 204.
15. Harada, N.; Nakanishi, K. *Circular Dichroic Spectroscopy - Exciton Coupling in Organic Stereochemistry*; University Science Books: Mill Valley, CA, 1983.
16. (a) Gawroński, J.K.; Połonski, T.; Lightner, D.A. *Tetrahedron* **1990**, *46*, 8053-8066.
    (b) Trull, F.R.; Shrout, D.P.; Lightner, D.A. *Tetrahedron* **1992**, *48*, 8189-8198.

(*Received in USA* 8 *February* 1996; *accepted* 11 *March* 1996)